

Reference dimensions of stented surgical aortic bioprostheses for valve size determination



Malcolm Anastasius¹, MBBS, MM, PhD; Marcelo Godoy¹, MD; Jonathan R. Weir-McCall², MBChB, PhD; Vinayak Bapat³, MD; Janarthanan Sathananthan¹, MBChB, MPH; Mark Hensey¹, MB, BCH, BAO; Stephanie L. Sellers⁴, PhD; Anson Cheung¹, MD; Jian Ye¹, MD; David A. Wood¹, MD; Jonathon Leipsic¹, MD, FSCCT; John Webb¹, MD; Philipp Blanke^{1*}, MD, FSCCT

1. Center for Heart Valve Innovation, St. Paul's Hospital and University of British Columbia, Vancouver, BC, Canada; 2. Department of Radiology, University of Cambridge, Papworth Hospital, Cambridge, United Kingdom; 3. Division of Cardiology, New York-Presbyterian Hospital, Columbia University Medical Center, New York, NY, USA; 4. Centre for Heart Lung Innovation and Department of Radiology, University of British Columbia and St. Paul's Hospital, Vancouver, BC, Canada

This paper also includes supplementary data published online at: <https://eurointervention.pconline.com/doi/10.4244/EIJ-D-19-00921>

Introduction

Aortic valve-in-valve (aVIV) procedures are advancing the management of failed bioprosthetic surgical heart valves (SHV)^{1,2}. As opposed to transcatheter heart valve (THV) replacement for native aortic stenosis, selection of the transcatheter THV size for aVIV procedures is based on the SHV size and not on anatomical measurements. However, accurate SHV size information may not be available in medical records. While computed tomography (CT) may be used to derive dimensions of the SHV, it does have limitations³. The aim of this study was to establish reference data for CT dimensions across commonly used aortic stented SHV types and sizes in order to determine the manufacturer's labelled size from a CT data set.

Material and methods

STUDY POPULATION

CT data sets of patients who underwent aVIV planning for failed SHV at St. Paul's Hospital (Vancouver, BC, Canada) between 2013 and 2018 were included. We also obtained 25 specimens

from the Cardiovascular Tissue Registry at the Centre for Heart Lung Innovation (University of British Columbia and St. Paul's Hospital), to provide a more complete representation of commonly encountered SHV (*ex vivo* imaging). The manufacturer's labelled SHV size was determined from medical records. The Research Ethics Board at the University of British Columbia/Providence Health Care approved this study.

See **Supplementary Appendix 1** for CT data acquisition and reconstruction, CT image and statistical analysis.

CT image analysis was performed as follows. First, the reconstruction phase with the best image quality was identified. Next, using multiplane reformats, a plane transecting the basal ring was created. Measurements were performed by fitting a circular region of interest to the centre of the radiopaque scaffold, to yield area and diameter.

Results

Average patient age at the time of CT imaging was 72±13 years; 101 (69%) patients were male. Median time between the initial

*Corresponding author: University of British Columbia, Department of Radiology, St. Paul's Hospital, 1081 Burrard St, Vancouver, BC V6Z 1Y6, Canada. E-mail: phil.blanke@gmail.com

SHV implantation and time of CT was 9.0 years (interquartile range 4 years).

Derivation of the study cohort is shown in **Figure 1**. CT appearance and alignment of the region of interest for measurement of SHV size are illustrated in **Figure 2**, for 10 common valve types. Measurement results are listed in **Table 1** and illustrated in **Figure 2** and **Figure 3**. There was excellent correlation between the CT-derived SHV size and the manufacturer size for all SHV (**Supplementary Appendix 2, Supplementary Figure 1, Supplementary Figure 2**).

Discussion

There is increasing adoption of aVIV procedures for patients with failed surgical aortic bioprosthetic valves, given growing evidence

that the procedure is safe and effective^{1,2}. In planning for an aVIV procedure, CT may be used for measurement of the SHV size.

For planning an aVIV procedure, existing SHV size information is essential for determining THV size⁴. Lack of SHV sizes in aVIV procedures can lead to incorrect THV size selection, resulting in either undersizing and paravalvular leak or device embolisation, or oversizing leading to incomplete THV expansion and high transprosthetic gradients¹. Patient SHV size documentation may be absent and thus determining SHV size from CT seems desirable, with CT imaging already required for aVIV planning⁵.

CT-based *in vivo* SHV sizing data are limited to a single study which evaluated SHV by measuring the inner contour of the basal sewing ring⁶. Importantly, the present study provides a more complete collection of valve types and sizes, and the measurement

Table 1. Reference chart of CT-derived SHV dimensions and manufacturers' labelled size.

Aortic SHV	Manufacturer ID (mm)	CT diameter (mm)	CT area (mm ²)	n
PERIMOUNT Magna Ease (Model 3300TFX) (Edwards Lifesciences, Irvine, CA, USA)	19	n/a	n/a	n/a
	21	20.4±0.4	327±10	5
	23	22.7±0.4	407±13	2
	25	24.5±0.5	472±17	10
	27	26.8±0.1	568±6	5
	29	28.9±0.2	610±110	5
PERIMOUNT Magna (Model 3000TFX) (Edwards Lifesciences)	19	n/a	n/a	n/a
	21	20.7±0.2	353±46	7
	23	22.6±0.3	401±8	9
	25	24.8±0.3	483±10	8
	27	26.8±0.3	570±13	8
	29	29.1±0.1	670±11	2
PERIMOUNT (Model 2900) (Edwards Lifesciences)	19	n/a	n/a	n/a
	21	20.8±0.5	341±12	6
	23	22.6±0.2	401±8	2
	25	24.6±0.3	476±138	6
	27	26.9±0.1	563±20	2
	29	n/a	n/a	n/a
Carpentier-Edwards supra-annular valve (Edwards Lifesciences)	19	n/a	n/a	n/a
	21	21.1±0.2	350±5	3
	23	23.1±0.2	419±6	5
	25	25.0±0.2	492±6	3
	27	27.1±0.2	578±7	4
	29	n/a	n/a	n/a
PERIMOUNT (Model 2700) (Edwards Lifesciences)	19	n/a	n/a	n/a
	21	20.7±0.2	340±5	5
	23	22.7±0.1	408±5	7
	25	25.1	496±2	1
	27	26.6±0.1	558±10	2
	29	n/a	n/a	n/a
Mosaic (Model 305) (Medtronic, Minneapolis, MN, USA)	19	n/a	n/a	n/a
	21	21.1	349	1
	23	22.7±0.1	406±5	5
	25	24.7±0.2	482±10	8
	27	26.9±0.2	570±7	6
	29	28.8±0.1	656±2	3
Mitroflow (Sorin Group, Saluggia, Italy)	19	n/a	n/a	n/a
	21	21.5±0.3	361±7	6
	23	23.4±0.3	431±12	15
	25	25.5±0.5	452±7	8
	27	27.4±0.02	596±2	2
	29	n/a	n/a	n/a
Trifecta (St. Jude Medical, St. Paul, MN, USA)	19	n/a	n/a	n/a
	21	20.5±0.04	333±2	7
	23	22.5±0.05	386±32	4
	25	24.6±0.1	477±5	2
	27	26.6±0.0	559±2	2
	29	28.5	642	1
Epic (St. Jude Medical)	19	n/a	n/a	n/a
	21	21.1	350±3	2
	23	22.7	404	1
	25	25.2±0.1	498±0	2
	27	26.8±0.1	559±3	2
	29	28.4	638	1
Hancock (Medtronic)	19	n/a	n/a	n/a
	21	n/a	n/a	n/a
	23	22.8±0.5	408±19	5
	25	25.1±0.1	496±3	2
	27	26.9	571	1
	29	29.2±0.2	672±8	2

CT area and diameter stratified by manufacturers' labelled SHV size. Data are presented as mean±SD. ID: internal diameter; n: number of valves studied; n/a: data not available

technique allows more robust translation to CT systems with different acquisition and reconstruction settings. We deliberately assessed CT dimensions along the centre of the radiopaque basal frame to reduce the impact of acquisition and reconstruction technique as well as artefacts.

CT-based SHV dimension assessment can be affected by artefacts due to the radiopaque component of the basal frame and sewing ring. These artefacts include blooming artefacts due to partial volume averaging as well as beam-hardening and streak artefacts. Blooming artefacts lead to overestimation of the metal component size, and thus to an underestimation when attempting to derive an internal diameter (ID) of the SHV from CT. Similarly, streak artefacts can impair accurate contour detection. Further, the extent of blooming and streak artefacts is influenced by tube potential, reconstruction technique and kernel, and window settings, as explained in **Supplementary Appendix 3**⁷. Given that these factors influence the appearance of metal components, assessment of an ID appears less robust. Instead, the technique employed in this study is independent of the above factors, by measuring along the centre of the visualised radiopaque basal frame.

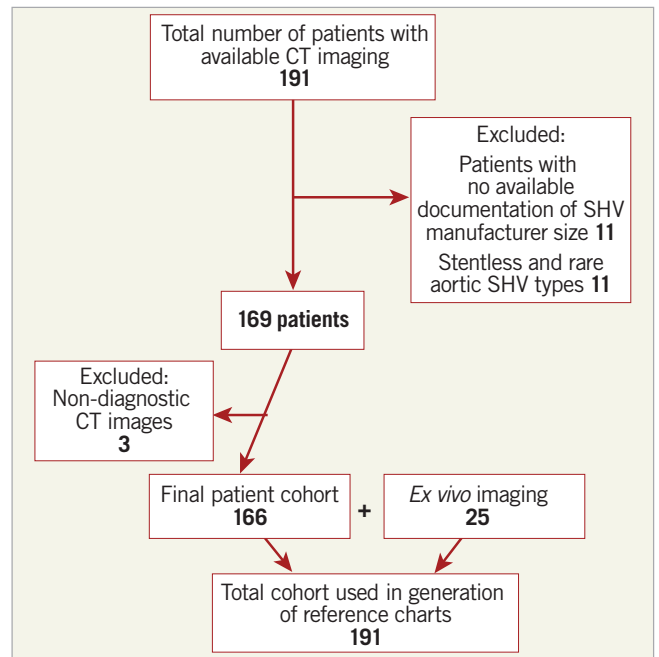


Figure 1. Flow diagram demonstrating patient inclusion and exclusion.

Valve	Volume-rendered reconstructions & measurement technique	CT appearance
Carpentier-Edwards supra-annular Valve (SAV) (Edwards Lifesciences)		Radiopaque Elgiloy metal wire stent, three posts and a discontinuous base. One wire connection at one base. Transition from valley to post smoother than in CE Standard.
PERIMOUNT 2700 (Edwards Lifesciences)		Radiopaque cobalt-chromium frame, three posts and a discontinuous base. One wire connection at one post apparent as asymmetric thickening of a single post.
PERIMOUNT (Model 2900) (Edwards Lifesciences)		Radiopaque undulating basal ring. Continuous thin stent frame above the base forming three radiopaque posts.
PERIMOUNT Magna (Model 3000TFX) (Edwards Lifesciences)		Radiopaque undulating basal ring with regular indentations. Continuous thin stent frame above the base forming three radiopaque posts.
PERIMOUNT Magna Ease (Model 3300TFX) (Edwards Lifesciences)		Radiopaque undulating basal ring with single indentation at peak. Continuous thin stent frame above the base forming three radiopaque posts.

Figure 2. Lateral and en face CT volume-rendered images and multiplanar reformats aligned with the basal SHV ring, demonstrating circular ROI measurement (red circle) centred within the radiopaque contour (bone window) for 5 commonly used SHVs.


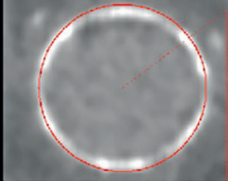

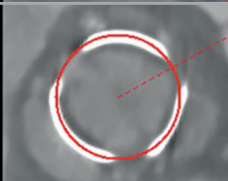
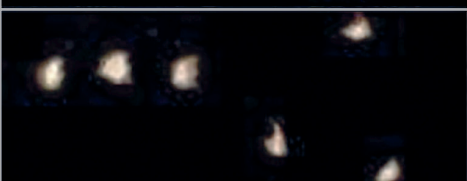


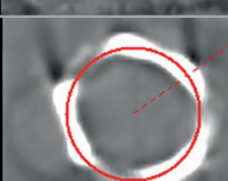
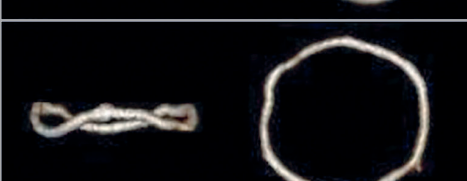
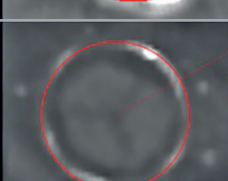
Valve	Volume-rendered reconstructions & measurement technique		CT appearance
Trifecta (St. Jude Medical)			Radiopaque titanium stent frame forming a three-pronged coronet with undulating base.
Hancock II (Medtronic)			Floating radiopaque markers at the top of radiolucent stent posts. Undulating radiopaque sewing ring.
Mosaic (Model 305) (Medtronic)			Floating radiopaque markers at the peak of radiolucent stent posts. Radiolucent sewing ring.
Mitroflow (Sorin)			Undulating radiopaque sewing ring, radiolucent stent posts.
Epic (St. Jude Medical)			Thin radiopaque sewing ring with one focal area which appears thicker (wire connector); radiolucent stent posts.

Figure 3. Lateral and en face CT volume-rendered images and multiplanar reformats aligned with the basal SHV ring, demonstrating circular ROI measurement (red circle) centred within the radiopaque contour (bone window) for 5 commonly used SHVs. Mosaic and Epic: measurement performed by fitting a circular ROI to the centre of the thin radiolucent sewing ring.

Measurement variability within individual valve type and size was limited. Only the Mitroflow SHV (Sorin Group, Saluggia, Italy) demonstrated higher measurement variability, due to the non-planar configuration of the basal ring. There was no overlap among assessed dimensions between different labelled valve sizes, permitting unambiguous determination of the labelled SHV size.

There is systematic discrepancy between the stent ID, defined as the inner diameter of the stent frame when covered with fabric or pericardium but without the valve leaflets, and the true ID, accounting for the valve leaflet insertions⁴. Importantly, CT does not appear capable of assessing the stent ID given the above-mentioned impact on assessing the inner frame contour, nor can CT assess the true ID, which can only be assessed on a bench top. Thus, in the authors' opinion, CT assessment should include a reproducible SHV size measurement, with subsequent comparison to a reference chart for determining the manufacturer's labelled valve size, which can then be used to ascertain the stent ID and true ID, and the appropriate THV size using existing resources⁸.

Study limitations

This is a single-centre study, with the available valve types and sizes limited to local practice. Older-generation SHVs not commonly encountered in current clinical practice, such as the Carpentier-Edwards standard were not included⁹. The mechanism of aortic SHV degeneration and presence of pannus were not taken into account in the CT measurement.

Conclusion

The study provides a comprehensive reference chart of CT-derived SHV dimensions to allow identification of the manufacturers' labelled size from CT measurements, and facilitate THV sizing for aVIV procedures.

Impact on daily practice

CT may be used to determine the manufacturers' labelled SHV size and guide aVIV procedural planning.

Acknowledgements

The authors wish to acknowledge the support provided by Drs Bruce McManus and Paul Hanson in the Cardiovascular Tissue Registry at St. Paul's Hospital.

Conflict of interest statement

J. Leipsic serves as a consultant and has stock options in HeartFlow and Circle Cardiovascular Imaging, institutional core laboratory agreements with Edwards Lifesciences, Abbott and Medtronic and receives speaking fees from GE Healthcare. J. Webb is a consultant to, and has received research funding from, Edwards Lifesciences, Abbott Vascular, Boston Scientific and ViVITRO Labs. D. Wood is a consultant to Edwards Lifesciences and receives grant support from Edwards Lifesciences, Abbott Vascular, AstraZeneca and Boston Scientific. J. Sathananthan has received speaking fees from and is a consultant to Edwards Lifesciences. P. Blanke is a consultant for Edwards Lifesciences and Circle Cardiovascular Imaging, and provides CT core lab services for Edwards Lifesciences, Medtronic, Neovasc, and Tendyne Holdings, for which he receives no direct compensation. V. Bapat is a consultant to Medtronic, Boston Scientific, Meril, 4C and Edwards Lifesciences. All other authors have reported that they have no relationships relevant to the contents of this paper to disclose.

References

1. Dvir D, Webb J, Brecker S, Bleiziffer S, Hildick-Smith D, Colombo A, Descoutures F, Hengstenberg C, Moat N, Bekeredjian R, Napodano M, Testa L, Lefevre T, Guetta V, Nissen H, Hernandez J, Roy D, Teles R, Segev A, Dumonteil N, Fiorina C, Gotzmann M, Tchetché D, Abdel-Wahab M, De Marco F, Baumbach A, Laborde J, Kornowski R. Transcatheter aortic valve replacement for degenerative bioprosthetic surgical valves: results from the global valve-in-valve registry. *Circulation*. 2012;126:2335-44.
2. Tuzcu EM, Kapadia SR, Vemulapalli S, Carroll JD, Holmes DR Jr, Mack MJ, Thourani VH, Grover FL, Brennan JM, Suri RM, Dai D, Svensson LG. Transcatheter Aortic Valve Replacement of Failed Surgically Implanted Bioprostheses: The STS/ACC Registry. *J Am Coll Cardiol*. 2018;72:370-82.
3. Rajani R, Attia R, Condemni F, Webb J, Woodburn P, Hodson D, Nair A, Preston R, Razavi R, Bapat VN. Multidetector computed tomography sizing of bioprosthetic valves: guidelines for measurement and implications for valve-in-valve therapies. *Clin Radiol*. 2016;71:e41-8.
4. Bapat VN, Attia R, Thomas M. Effect of valve design on the stent internal diameter of a bioprosthetic valve: a concept of true internal diameter and its implications for the valve-in-valve procedure. *JACC Cardiovasc Interv*. 2014;7:115-27.
5. Blanke P, Weir-McCall JR, Achenbach S, Delgado V, Hausleiter J, Jilaihawi H, Marwan M, Norgaard BL, Piazza N, Schoenhagen P, Leipsic JA. Computed tomography imaging in the context of transcatheter aortic valve implantation (TAVI) / transcatheter aortic valve replacement (TAVR): An expert consensus document of the Society of Cardiovascular Computed Tomography. *J Cardiovasc Comput Tomogr*. 2019;13:1-20.
6. Sucha D, Symersky P, Tanis W, Mali WP, Leiner T, van Herwerden LA, Buddle RP. Multimodality Imaging Assessment of Prosthetic Heart Valves. *Circ Cardiovasc Imaging*. 2015;8:e003703.
7. Kalisz K, Buehe F, Saboo SS, Abbara S, Halliburton S, Rajiah P. Artifacts at Cardiac CT: Physics and Solutions. *Radiographics*. 2016;36:2064-83.
8. Bapat V. Valve-in-valve apps: why and how they were developed and how to use them. *EuroIntervention*. 2014;10:U44-51.
9. Jamieson WR, Burr LH, Junsz MT, Munro AI, Hayden RI, Miyagishima RT, Ling H, Fradet GJ, Lichtenstein SV, Stewart KM. Carpentier-Edwards standard and supraannular porcine bioprostheses: comparison of technology. *Ann Thorac Surg*. 1999;67:10-7.

Supplementary data

Supplementary Appendix 1. Methods.

Supplementary Appendix 2. Results.

Supplementary Appendix 3. Discussion.

Supplementary Figure 1. Graphs of measurements stratified by valve type and size.

Supplementary Figure 2. Bland-Altman plot of CT-based measurement of SHV size (diameter) for two clinician observers in a subgroup of the study cohort (n=75).

The supplementary data are published online at:
<https://eurointervention.pcronline.com/doi/10.4244/EIJ-D-19-00921>



Supplementary data

Supplementary Appendix 1. Methods

Study population

CT data sets of patients who underwent planning for a potential aVIV procedure for a failed SHV at St. Paul's Hospital (Vancouver, BC, Canada) between October 2013 and December 2018 were included (in vivo imaging). We also obtained 25 specimens from the Cardiovascular Tissue Registry at the Centre for Heart Lung Innovation (University of British Columbia and St. Paul's Hospital), to provide a more complete representation of commonly encountered SHVs (ex vivo imaging). The Research Ethics Board at the University of British Columbia/Providence Health Care approved this study. Medical records for all patients were reviewed to determine SHV type and manufacturer's labelled SHV size recorded at the time of original surgical bioprosthetic valve replacement. Only patients with stented valves were included.

Patients with an unknown valve type or size, rare valve types that did not sufficiently cover the currently employed valve sizes, or incomplete documentation, were excluded from this analysis. Patients with stentless valves were excluded, given the absence of radiopaque structures for CT measurement as well as variable configuration due to the lack of a rigid scaffold (**Figure 1**).

CT data acquisition and reconstruction

CT images of surgical heart valves were acquired using a wide detector CT scanner (GE Revolution or GE 750HD; General Electric, Milwaukee, WI, USA). CT images were acquired and reconstructed according to current guidelines [5], employing retrospective ECG gating, thin-sliced collimation of 0.625 mm, 120 kVP tube voltage and tube current adjusted to body habitus. Images were reconstructed as multiphase data sets in 10% intervals using a soft-tissue convolution kernel. Ex vivo specimens were scanned using similar acquisition and reconstruction parameters, without ECG gating.

Contrast-enhanced CT images, obtained as part of recommended routine planning of aVIV procedures, were used for assessment of SHV size. However, in the presence of

a contraindication to contrast, a non-contrast CT study may have been used to fit a region of interest to the centre of the radiopaque scaffold for measurement of SHV size.

CT image analysis

CT images were analysed using commercially available post-processing software iNtuition (TeraRecon, Foster City, CA, USA). Observers were blinded to the manufacturers' labelled SHV size. Analysis was performed as follows. First, the reconstruction phase with the best image quality, i.e., the least motion artefacts and sharpest basal ring contours were identified. Using multiplane reformats, a plane transecting the basal ring was created by manipulating the crosshairs in the corresponding views. For non-planar basal rings, a plane demonstrating the most complete basal ring was identified. Window levels were adjusted to a standard bone window, defined by a window level of 800 HU and a width of 2,000 HU, for measurement with reduced metal blooming. Measurements were performed by fitting a circular region of interest to the centre of the radiopaque scaffold, i.e., centred between the inner and outer contours of the radiopaque scaffold. The circular region yielded area (in mm²) and diameter (mm). Measurements were performed three times with subsequent averaging of values in order to mitigate measurement error.

Statistical analysis

All continuous variables are expressed as mean±SD. Variables with non-normal distributions are presented as median with range. Pearson's correlations were used to test association between CT measurements and manufacturers' labelled SHV size. Intraclass correlation was performed to determine interobserver variability, and Bland-Altman analyses for comparison of CT SHV size measurement between two clinician observers. Statistical analysis was performed using Prism 7 (GraphPad Software, San Diego, CA, USA).

Supplementary Appendix 2. Results

Across all valve sizes, the mean difference between the manufacturers' labelled SHV size and the CT assessed diameter of the circular ROI was -0.3 ± 0.2 mm for PERIMOUNT Magna Ease, -0.2 ± 0.2 mm for PERIMOUNT Magna, -0.3 ± 0.2 mm for

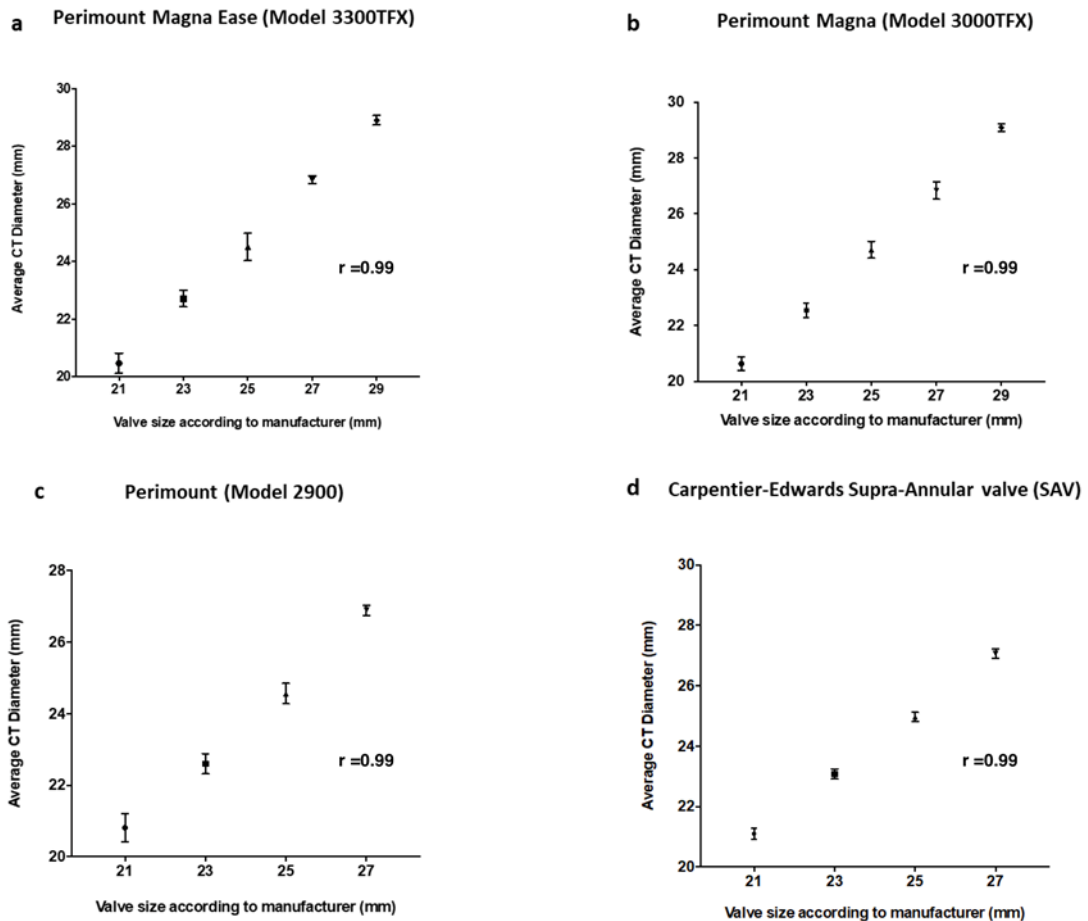
PERIMOUNT, -0.2 ± 0.2 mm for Mosaic, -0.5 ± 0.1 mm for Trifecta, 0.5 ± 0.1 mm for Mitroflow, 0.1 ± 0.1 mm for CE SAV, -0.2 ± 0.3 mm for Epic, -0.4 ± 0.4 mm for PERIMOUNT 2700, and 0 ± 0.2 mm for Hancock.

Two CT imaging clinicians independently performed CT measurements for a subgroup of 75 SHVs, yielding an intraclass correlation coefficient of 0.99, indicating good interobserver variability. Bland-Altman analysis showed good agreement between clinicians (**Supplementary Figure 2**).

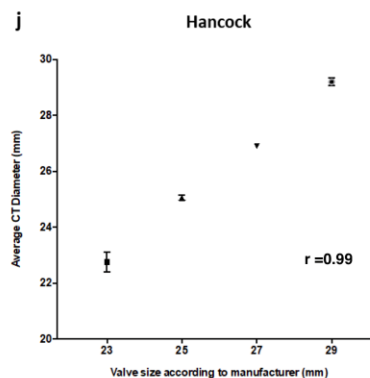
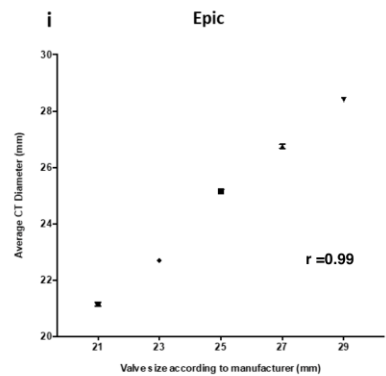
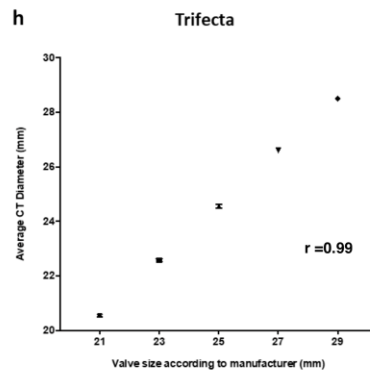
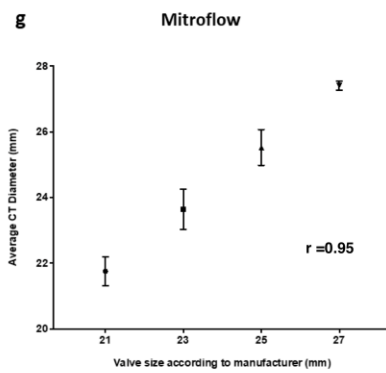
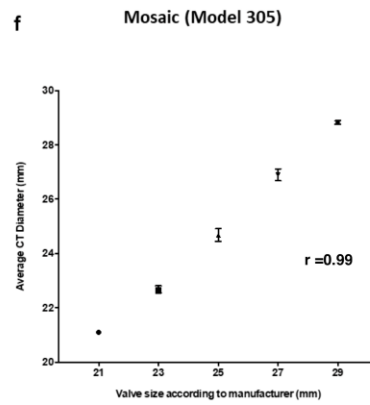
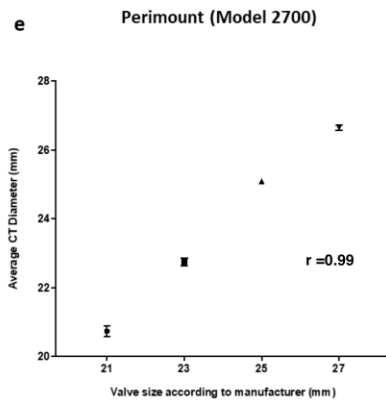
Supplementary Appendix 3. Discussion

For measurements, we deliberately assessed CT dimensions along the centre of the visualised, radiopaque basal frame, in order to reduce the impact of acquisition and reconstruction technique as well as artefacts. CT-based assessment of SHV dimension can be affected by artefacts caused by the radiopaque component of the basal frame and sewing ring of stented SHVs. These artefacts include blooming artefacts due to partial volume averaging as well as beam-hardening and streak artefacts.

In CT imaging of SHVs, the extent of blooming and streak artefacts is influenced by the following [7]: 1) tube potential, with less artefact and less blooming at higher tube voltage; 2) reconstruction technique, with less artefact with higher degree of iterative reconstruction or use of a monoenergetic image at higher energy levels; 3) reconstruction kernel, with less artefact when using a harder kernel, i.e., a stent kernel, compared to a standard soft-tissue convolution kernel; 4) window setting at time of image assessment, with less depiction of artefact when using a large width window, such as a “bone” window. Given that these factors influence the appearance of the metal components, assessment of an internal diameter appears less robust. Instead, the technique employed in this study, namely purposefully measuring along the centre of the visualised radiopaque basal frame, allows relative independence from the above-listed factors.

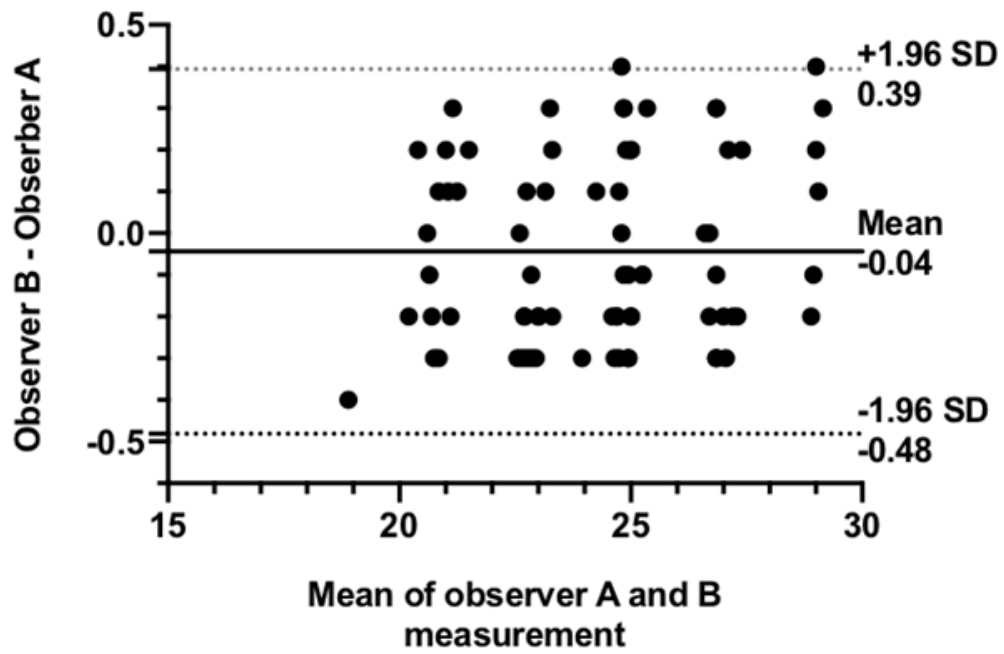


Supplementary Figure 1. Graphs of measurements stratified by valve type and size. Graphs of CT-derived SHV size versus manufacturers' labelled SHV, for (a) PERIMOUNT Magna Ease (Model 3300TFX) (Edwards Lifesciences), (b) PERIMOUNT Magna (Model 3000TFX) (Edwards Lifesciences), (c) PERIMOUNT (Model 2900) (Edwards Lifesciences), (d) Carpentier-Edwards (CE) standard supra-annular valve (SAV) (Edwards Lifesciences),



Supplementary Figure 1 (continued).

(e) PERIMOUNT (Model 2700) (Edwards Lifesciences), (f) Mosaic (Model 305) (Medtronic), (g) Mitroflow (Sorin), (h) Trifecta (St. Jude Medical), (i) Epic (St. Jude Medical), (j) Hancock (Medtronic). Data are presented as mean \pm SD. CT: computed tomography. Pearson's correlation coefficient (r) is presented for each graph.



Supplementary Figure 2. Bland-Altman plot of CT-based measurement of SHV size (diameter) for two clinician observers in a subgroup of the study cohort (n=75).